

# Convection in radiatively inefficient back hole accretion flows

Igor V. Igumenshchev\* and Marek A. Abramowicz†

\**Institute of Astronomy, 48 Pyatnitskaya Ulitsa, 109017 Moscow, Russia*

†*Department of Astronomy & Astrophysics, Göteborg University & Chalmers University of Technology, 412-96 Göteborg, Sweden*

**Abstract.** Recent numerical simulations of radiatively inefficient accretion flows onto compact objects have shown that convection is a general feature in such flows. Dissipation of rotational and gravitational energies in the accretion flows results in inward increase of entropy and development of efficient convective motions. Convection-dominated accretion flows (CDAFs) have a structure that is modified significantly in comparison with the canonical advection-dominated and Bondi-like accretion flows. The flows are characterized by the flattened radial density profiles,  $\rho(R) \propto R^{-1/2}$ , and have reduced mass accretion rates. Convection transports outward a significant amount of the released binding energy of the accretion flow. We discuss basic dynamical and observational properties of CDAFs using numerical models and self-similar analytical solutions.

## INTRODUCTION

Observations of accreting black holes of different mass, from the stellar mass black holes to the supermassive black holes in the center of galaxies, show impressive similarities of data, which point at identical physical processes in accreting plasma. Also, black hole candidates demonstrate a great variety of physical conditions in the flows and, possibly, existence of a variety of accretion regimes. Existing theories describe different regimes of black hole accretion flows, which can be realized under different physical conditions. If matter accretes with a low specific angular momentum,  $j \ll R_g c$ , it forms spherical flows, which are described by Bondi solution [1] in the case of adiabatic flows. Here  $R_g$  is the gravitational radius of the black hole, and  $c$  is the speed of light. If matter has a large specific angular momentum,  $j \gg R_g c$ , then accretion disks are formed. The structure of accretion disks crucially depends on the efficiency of radiative cooling. If matter radiates efficiently, i.e. the radiative cooling time is shorter than the accretion time,  $t_{rad} \ll t_{accr}$ , the disks are geometrically thin,  $H \ll R$ , where  $H$  is the scale height of the flow, and  $R$  is the corresponding radius. The radial structure of such disks is described by the Shakura & Sunyaev model [2]. In the case of radiatively

inefficient flows,  $t_{rad} \gg t_{accr}$ , the internal energy of accreting matter is close to the virial energy, and the formed disks are geometrically thick,  $H \sim R$ . The thick disks can be formed in two limiting cases of very high,  $\dot{M} \gg L_{Edd}/c^2$ , and very low,  $\dot{M} \ll L_{Edd}/c^2$ , accretion rates, where  $L_{Edd}$  is the Eddington luminosity of the black hole. In the former case, the optical depth of accretion flow is very large, and photons, which carry most of the internal energy, are trapped inside the inflowing matter and can not be radiated away. In the latter case, the accreting plasma is very diluted, so that different radiative mechanisms are inefficient to cool plasma on the accretion time scales. A model which describes the geometrically thick accretion disks was called the advection-dominated accretion flow (ADAF) and attracted a considerable attention during the last two decades [3–10]. The main feature of ADAFs is that most of the locally released gravitational and rotational energies of accretion flow is advected inward in the form of the gas internal energy, and the latter is finally absorbed by the black hole. The recent interest to ADAFs was generated mostly by attempts using this model to explain the low-luminosity X-ray objects of both galactic and intergalactic nature (for recent reviews see [11,12]).

## ADVECTION-DOMINATED FLOWS

Properties of ADAFs could be better understood by analyzing the self-similar solution of the height-integrated hydrodynamical equations [10]. The solution depends on two parameters, the viscosity parameter  $\alpha$  and the adiabatic index  $\gamma$ , and satisfies the following scalings for the density  $\rho$ , the radial velocity  $v_R$ , the angular velocity  $\Omega$ , the isothermal sound speed  $c_s$  and  $H$ :

$$\begin{aligned}
 \rho(R) &\propto R^{-3/2}, \\
 v_R(R) &\propto R^{-1/2}, \\
 \Omega(R) &\propto R^{-3/2}, \\
 c_s(R) &\propto R^{-1/2}, \\
 H(R) &= c_s/\Omega_K \propto R,
 \end{aligned}
 \tag{1}$$

where  $\Omega_K$  is the Keplerian angular velocity. Because of neglect of the radiative energy losses of the flow, the flow structure is independent of the mass accretion rate  $\dot{M}$ . The accretion rate determines only scales of density through the relation  $\rho = \dot{M}/(4\pi R H v_R)$ .

Two inconsistencies were found related to the model of ADAFs. The first is that ADAFs must be convectively unstable [4,5,7]. The second is connected to the positiveness of “Bernoulli parameter” in ADAFs [9],

$$Be = \frac{v_R^2}{2} + W - \frac{GM}{R} > 0,$$

where  $W$  is the specific enthalpy. A hypothesis was proposed that the latter problem could be solved by assuming the presence of powerful bipolar outflows in the accretion flows [13,14]. However, according to the later investigations [15,16], the hypothesis met some difficulties. The consequences of the earlier mentioned inconsistencies for ADAFs was understood after performing two- and three-dimensional hydrodynamic simulations of the inefficiently radiative accretion flows [17–22]. The simulations have revealed a new accretion regime of inefficiently radiated plasma, in which convection plays a dominant role determining structure and dynamics of the flow. Such a regime we shall refer as CDAF, the convection-dominated accretion flow.

## CONVECTION INSTABILITY

Behavior of convective blobs in non-rotating medium depends sensitively on the superadiabatic gradient

$$\Delta\nabla c_s^2 = -c_s^2 \frac{d}{dR} \ln \left( \frac{P^{1/\gamma}}{\rho} \right),$$

which determines the Brunt-Väisälä frequency  $N$  given by

$$N^2 = -\frac{g_{eff}}{c_s^2} \Delta\nabla c_s^2,$$

where  $g_{eff} = -(1/\rho)(dP/dR)$  is the radial effective gravity. When  $N^2$  is positive, perturbations of the blobs have an oscillatory behavior with the frequency  $N$  and the medium is convectively stable. However, when  $N^2$  is negative, perturbations have a runaway growth, leading to convection. Convection is present whenever  $\Delta\nabla c_s^2$  is positive, i.e. when the entropy gradient, given by

$$T \frac{ds}{dR} = -\frac{\gamma}{\gamma - 1} \Delta\nabla c_s^2,$$

is negative. This is the well-known Schwarzschild criterion.

When there is rotation, a new frequency enters the problem and convection is no longer determined purely by the Brunt-Väisälä frequency. In this case, the effective frequency  $N_{eff}$  of convective blobs is given by

$$N_{eff}^2 = N^2 + \kappa^2,$$

where  $\kappa$  is the epicyclic frequency; for  $\Omega \propto R^{-3/2}$ , we have  $\kappa = \Omega$ . Again, when  $N_{eff}^2$  is negative, the rotating flows are convectively unstable.

When convection is developed, the convective blobs carry outward some amount of thermal energy. Under certain approximations (see details in [24]) the convective energy flux can be expressed in the form,

$$F_{conv} = -\nu_{conv}\rho T \frac{ds}{dR}, \quad (2)$$

where  $s$  is the specific entropy,  $T$  is the temperature,  $\nu_{conv}$  is the diffusion coefficient, defined by  $\nu_{conv} = (L_M^2/4)(-N_{eff}^2)^{1/2}$ , and  $L_M$  is the characteristic mixing-length. The coefficient  $\nu_{conv}$  can also be expressed in the  $\alpha$ -parameterization form,  $\nu_{conv} = \alpha_{conv}c_s^2/\Omega_K$ , where  $\alpha_{conv}$  is a dimensionless parameter that describes the strength of convective diffusion; this parameter is similar to the usual Shakura & Sunyaev  $\alpha$ .

In the case of the self-similar ADAF solution (1), calculations lead to the conclusion that  $N_{eff}^2 < 0$ , i.e. ADAFs are convectively unstable and must have the outward energy fluxes defined by equation (2).

## NUMERICAL RESULTS

To describe the results of numerical simulations of radiatively inefficient accretion flows, we shall mainly follow [21,22]. In these works the accretion flows were simulated by solving the nonrelativistic, time-dependent Navier-Stokes equations with thermal conduction,

$$\begin{aligned} \frac{d\rho}{dt} + \rho\nabla\mathbf{v} &= 0, \\ \rho\frac{d\mathbf{v}}{dt} &= -\nabla P + \rho\nabla\Phi + \nabla\mathbf{\Pi}, \\ \rho\frac{de}{dt} &= -P\nabla\mathbf{v} - \nabla\mathbf{q} + Q, \end{aligned} \quad (3)$$

where  $e$  is the specific internal energy,  $\Phi$  is the gravitational potential of the black hole,  $\mathbf{\Pi}$  is the viscous stress tensor with all components included,  $\mathbf{q}$  is the heat flux density due to thermal conduction and  $Q$  is the dissipation function. No radiative cooling was assumed and the ideal gas equation of state,  $P = (\gamma - 1)\rho e$ , was adopted. Only the shear viscosity was considered,

$$\nu = \alpha c_s^2/\Omega_K, \quad (4)$$

where  $\alpha$  is a constant,  $0 < \alpha \leq 1$ .

In the simulations, it was assumed that mass is steadily injected into the calculation domain from an equatorial torus near the outer boundary. Matter is injected with almost Keplerian angular momentum. Owing to viscous spread, a part of the injected matter moves inward and forms an accretion flow. The computations were started from an initial state in which there is a small amount of mass in the domain. After a time comparable to the viscous timescale, the accretion flow achieves a quasi-stationary behavior.

Results obtained by using two-dimensional axisymmetric simulations are summarized in Figure 1. Four types of accretion flows can be distinguished from the models with no thermal conduction (see Figure 1, left panel).

1. Convective flows. For a very small viscosity,  $\alpha \lesssim 0.03$ , accretion flows are convectively unstable. Axially symmetric convection transports the angular momentum *inward* rather than outward. Convection governs the flow structure, making a flattened density profile,  $\rho(R) \propto R^{-1/2}$ , with respect to the one for ADAFs. Convection transports a significant amount (up to  $\sim 1\%$ ) of the dissipated binding energy outward. No powerful outflows are present.

2. Large-scale circulations. For a larger, but still small viscosity,  $\alpha \sim 0.1$ , accretion flows could be both stable or unstable convectively, depending on  $\alpha$  and  $\gamma$ . The flow pattern consists of the large-scale ( $\sim R$ ) meridional circulations. No powerful unbound outflows are presented. In some respect this type of flow is the limiting case of the convective flows in which the small-scale motions are suppressed by larger viscosity.

3. Pure inflows. With an increasing viscosity,  $\alpha \simeq 0.3$ , the convective instability dies off. Some models (with  $\gamma \simeq 3/2$ ) are characterized by a pure inflow pattern, and agree in many respects with the self-similar ADAFs. No outflows are present.

4. Bipolar outflows. For a large viscosity,  $\alpha \simeq 1$ , accretion flows differ considerably from the simple self-similar models. Powerful unbound bipolar outflows are present.

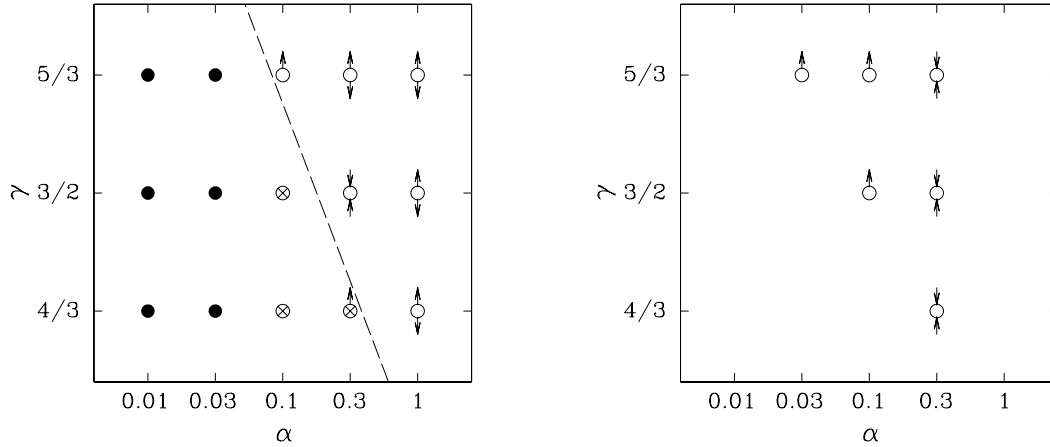


**FIGURE 1.** Properties of two-dimensional axisymmetric models of accretion flows. Models with no thermal conduction are shown in the left panel. Models with thermal conduction (Prandtl number  $\mathbf{Pr} = 1$ ) are shown in the right panel. Each circle represents a model in the  $(\alpha, \gamma)$  parameter space. The empty circles correspond to laminar flows, the crossed circles represent unstable models with large-scale ( $\sim R$ ) meridional circulations and solid circles indicate convective models. Two outward directed arrows correspond to bipolar outflows, whereas one arrow corresponds to a unipolar outflow. Two inward directed arrows correspond to a pure inflow. The dashed line on the left-hand panel approximately separates regions of convectively stable/unstable flows.

Figure 2 illustrates the density distribution and flow pattern in the low viscosity models. The models show complicated time-dependent behavior with numer-

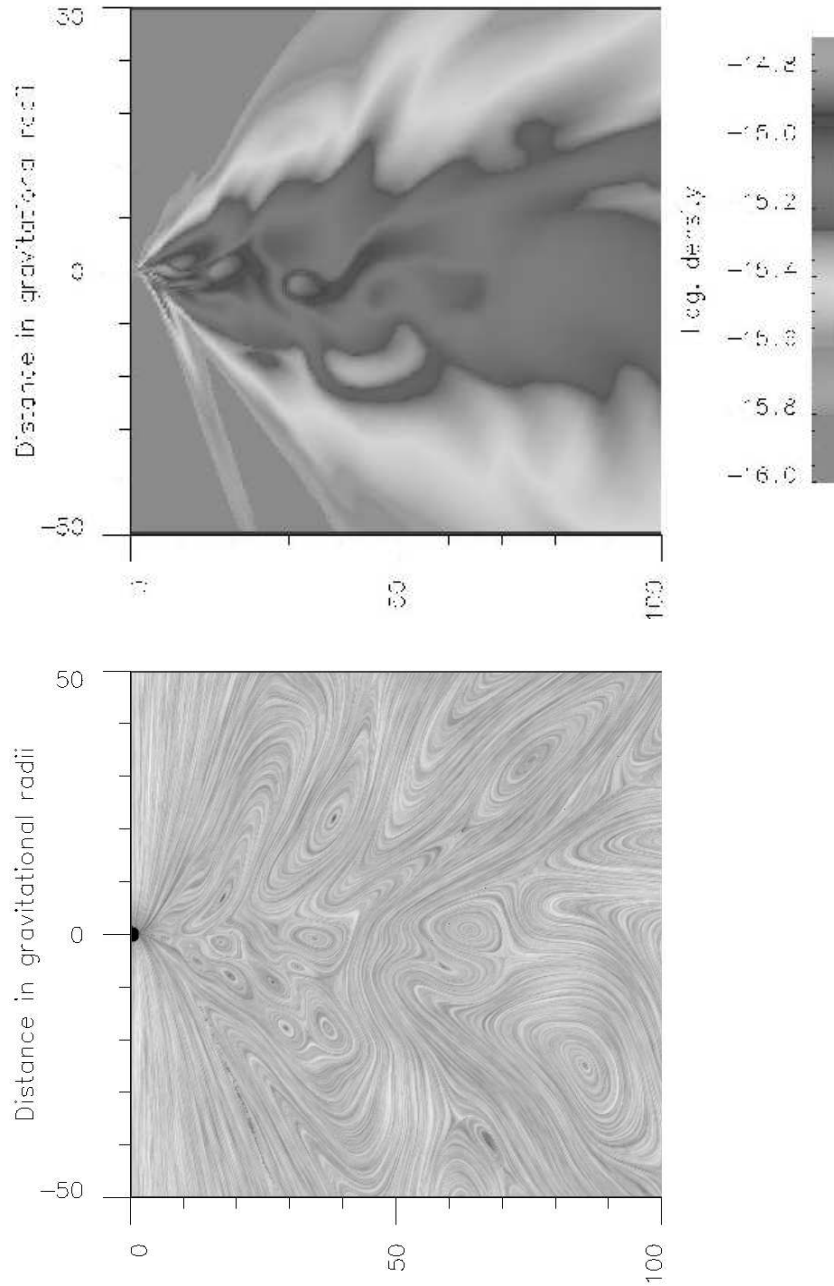


**FIGURE 2.** Snapshots of density distribution (upper panel) and streamlines (lower panel) from two-dimensional model of CDAF with  $\alpha = 0.01$  and  $\gamma = 5/3$ , in the meridional cross-section. The black hole is located at the origin. The flow pattern is highly time dependent and consists of numerous vortices of different spatial scales. The variability of flow pattern is accompanied by density variations and results in variability of the accretion rate.

ous vortices and circulations, and with density fluctuations. However, the time-averaged flow patterns are smooth and do not demonstrate small-scale features. Figure 3 shows typical behavior of radial profiles of variety of time- and angle-averaged variables in convective models. Except near the inner and outer boundaries ( $R < 10R_g$  and  $R > 10^3R_g$ ), the profiles of  $\rho$ ,  $c_s$ ,  $v$  and  $\Omega$  show prominent power-law behaviors.

Two-dimensional models have demonstrated that the  $(r, \varphi)$ -component of the volume averaged Reynolds stress tensor takes negative values in the case of convective flows. This means that axisymmetric convection transports the

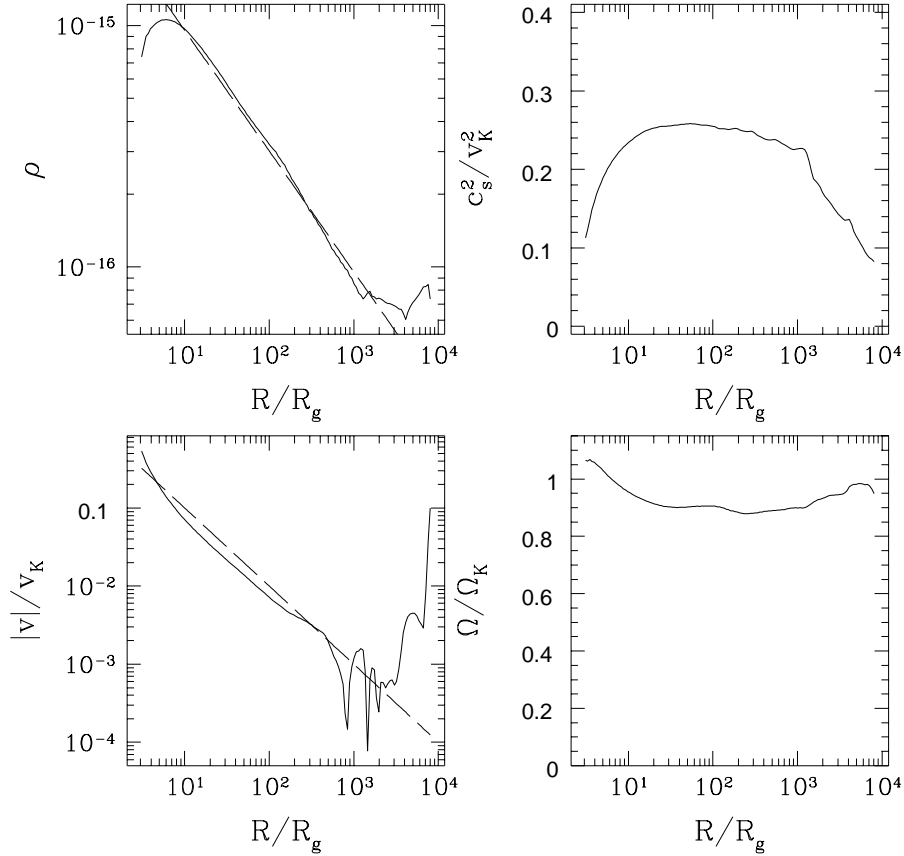


**FIGURE 3.** Selected properties of two-dimensional axisymmetric model with  $\alpha = 0.01$  and  $\gamma = 5/3$  [23]. All quantities have been averaged over polar angle  $\theta$  and time. Except near the boundaries ( $R < 10R_g$  and  $R > 10^3R_g$ ), the profiles of  $\rho$ ,  $c_s^2/v_K^2$ , and  $\Omega/\Omega_K$  show the power-law behaviors predicted by the self-similar convective envelope solution. In the upper left panel the dashed line corresponds to the analytical scaling  $\rho \propto R^{-1/2}$ . Similarly, in the lower left panel the dashed line corresponds to the expected scaling  $v \propto R^{-3/2}$  for CDAFs.

angular momentum inward. Indeed, if there are no azimuthal gradients of pressure, the turbulence attempts to erase the angular momentum gradient, which for the Keplerian-like angular velocity,  $\Omega \propto R^{-3/2}$ , means that the angular momentum transports inward. However, this is a property of axisymmetric flows. Does convection in real three-dimensional flows move angular momentum inward? Do such flows have significant azimuthal perturbations which destroy axisymmetry? The answer to this question has been found with the help of fully three-dimensional simulations, without the limiting assumption of axisymmetry [21]. The simulations have demonstrated a good qualitative and quantitative coincidence of the results of two- and three-dimension modeling. It was demonstrated that in the differentially rotating flows with nearly Keplerian angular velocities, all azimuthal gradients are efficiently washed out, leading to almost axisymmetrical structure of three-dimensional flows. Figure 4 illustrates axisymmetric structure of the low-viscosity accretion flow obtained in three-dimensional simulations.

All low-viscosity models have negative volume-averaged  $Be$  in all ranges of the

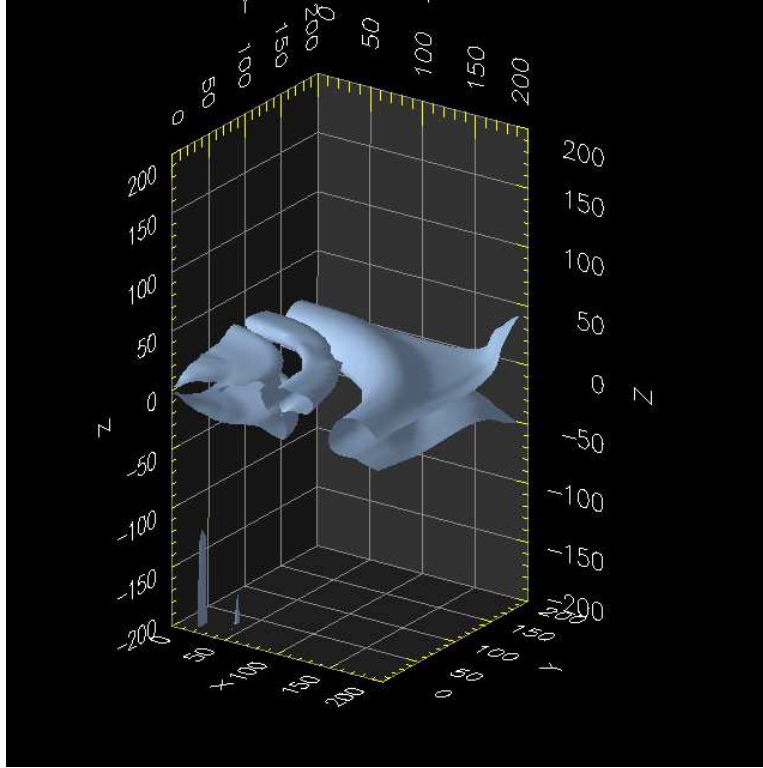


**FIGURE 4.** Snapshot of surfaces of a constant density in three-dimensional model of CDAF with  $\alpha = 0.01$  and  $\gamma = 5/3$ . Only a quarter of the innermost region of the full domain is shown. Accretion matter rotates around  $z$ -axis. The black hole is located at the origin. All axes are labeled in the units of  $R_g$ . One can clearly see that density perturbations, associated with motion of convective blobs in the accretion flow, have axially symmetric form with respect to the axis of rotation.



radii. Only temporal convective blobs and narrow regions at the disk surfaces show positive  $Be$ . It seems that the outward directed convection energy transport provides an additional cooling mechanism of the flows that always results in averaged  $Be < 0$ , opposite to positive  $Be$  obtained in ADAFs.

In several axisymmetric simulations, effects of turbulent thermal conduction have been studied. It was found that the conduction has an important influence on the flow structure, but it does not introduce a new type of flow in addition to those already discussed (see Figure 1, right panel). The conduction leads to a suppression of small-scale convection in the low-viscosity models. In the moderate-viscosity models the thermal conduction acts as a cooling agent in the outflows, reducing or even suppressing them.

Obtained properties of CDAF can have important implications for the spectra and luminosities of accreting black holes [20,22,23]. Indeed, since  $\rho \propto R^{-1/2}$  and  $T \propto R^{-1}$ , the bremsstrahlung cooling rate per unit volume varies as  $Q_{br} \propto \rho^2 T^{-1/2} \propto R^{-3/2}$ . After integration of  $Q_{br}$  over bulk of the flow one obtains the bremsstrahlung luminosity  $L_{br} \propto R$ . This means that CDAFs mostly radiate on the outside, whereas most of the radiative energy of ADAFs comes from the innermost region [10].

## SELF-SIMILAR CONVECTIVE ENVELOPE

Numerical simulations of convective accretion flows have been understood qualitatively after construction of analytical self-similar solutions of such types of flows [24,25]. In the presence of convection, the height-integrated angular momentum and energy equations can be written as follows,

$$J_{adv} + J_{visc} + J_{conv} = 0, \quad (5)$$

$$\rho RT \frac{ds}{dR} + \frac{1}{R^2} \frac{d}{dR} (R^2 F_{conv}) = \Omega (J_{visc} + J_{conv}), \quad (6)$$

where  $J_{adv}$ ,  $J_{visc}$  and  $J_{conv}$  are the advective, viscous and convective angular momentum fluxes respectively. Solutions of equations (5) and (6), together with the equation of motion in the radial direction, crucially depend on the direction of convective angular momentum transport. There are two extreme possibilities. The first one is that convection behaves like normal viscosity,

$$J_{conv} = -\nu_{conv} \rho R^3 (d\Omega/dR). \quad (7)$$

An alternative possibility is that the convective flux is directed down the specific angular momentum gradient,

$$J_{conv} = -\nu_{conv} \rho R [d(\Omega R^2)/dR]. \quad (8)$$

For  $\Omega \propto R^{-3/2}$ , convective fluxes (7) and (8) correspond to outward and inward transport of angular momentum respectively. Numerical simulations have demonstrated that  $J_{conv} < 0$  in CDAFs.

Choosing the convective flux (8) one can construct a *nonaccreting* solution with  $v_R = 0$ . We refer to it as a “convective envelope”. For this solution, from equation (5) one obtains  $J_{adv} = 0$  and  $J_{conv} = -J_{visc}$ . The latter means that in the convective envelopes the net angular momentum flux vanishes: the inward convective flux is exactly balanced by the outward viscous flux. Because of absence of advection (due to  $v_R = 0$ ) and zero local dissipation rate (due to zero net angular momentum flux), the energy equation (6) is satisfied trivially with  $F_{conv}(R) \propto R^{-2}$ . Finally, the convective envelope solution has the following scalings:

$$\begin{aligned} \rho(R) &\propto R^{-1/2}, \\ v_R(R) &= 0, \\ \Omega(R) &\propto R^{-3/2}, \\ c_s(R) &\propto R^{-1/2}, \\ H(R) &\propto R, \end{aligned} \tag{9}$$

The outward energy flux  $F_{conv}$  corresponds to luminosity  $L_{conv} = 4\pi R H F_{conv}$ , which is independent of radius. Source of this energy flux is formally located at  $R = 0$ , but the nature of the source is not specified in the self-similar solution. In more realistic CDAFs, the mass accretion rate  $\dot{M}$  is small, but it is not exactly zero. The fraction of the binding energy of the accreted mass released in the innermost region is the source of the energy required to support convection. In the case of CDAFs the convective luminosity can be expressed in the following form,  $L_{conv} = \varepsilon \dot{M} c^2$ , where the parameter  $\varepsilon$  has been estimated in numerical simulations,  $\varepsilon \simeq 0.01$ . A non-zero  $\dot{M}$  leads to a finite  $v_R = \dot{M}/(4\pi R H \rho) \propto R^{-3/2}$ . The latter scaling and the scalings of other quantities in (9) agree quite well with the numerical results (see Figure 3).

## RECENT MHD SIMULATIONS

There is good reason to believe that “viscosity” in differentially rotating accretion flows is produced by magnetic stress generated by the magneto-rotational instability (MRI) [26]. MHD simulations of accretion flows under conditions, in which CDAFs could be formed, have been recently performed ([27–32] and Matsumoto et al. in this Proceedings). A general conclusion of these studies is that MRI, and probably other instabilities of magnetized medium, leads to development of turbulence in accretion flows. The turbulence re-distributes angular momentum in the flows with an effective  $\alpha_{eff} \sim 0.01 - 0.1$ . The simulations show a tendency for density profiles in accretion flows to be flatter, than those in ADAFs.

In general, these results of MHD simulations do not contradict the results of hydrodynamical simulations of convective flows, which were discussed in previous sections. The MHD simulations have demonstrated the range of  $\alpha_{eff}$ , in which hydrodynamical models are convectively unstable. The flattened density profiles in MHD models are in good agreement with those found in convective hydrodynamical models. However, a direct comparison of results of both approaches meets difficulties. The main problem is a low spatial resolution, and as a consequence, a small radial range of flow patterns studied in the discussed MHD simulations. In this case of small radial ranges the effects of boundaries become significant enough to influence the flow structure. Thus, more powerful computers and more developed numerical codes are required to obtain a comparable spatial resolution to that used in hydrodynamical simulations.

Another problem which can introduce difficulties for the comparison is that some MHD simulations have uncontrolled losses of energy due to numerical reconnection of magnetic lines. These energy losses can artificially suppress convection in the considered flows and change the flow structures, independently of the used spatial resolution. The problem could be solved by using an “artificial” resistivity in MHD schemes (see [32] for detailed discussion).

## CONCLUSIONS

- Radiatively inefficient hydrodynamical black hole accretion flows with small viscosity ( $\alpha \lesssim 0.1$ ) are always dominated by convection. Thus for low viscosity flows the concept of ADAF is unphysical.
- At present, CDAFs provide the best theoretical model for understanding of radiatively inefficient, low viscosity accretion flows.
- CDAFs are hot, their thermal energy is close to the virial energy. They have relatively reduced mass accretion rate. The density distribution in CDAFs is flattened, comparing to the one in ADAFs and Bondi-like flows ( $\rho \propto R^{-1/2}$  in the former case vs.  $\rho \propto R^{-3/2}$  in the latter case). Convection transports outward a significant amount (up to  $\sim 1\%$ ) of dissipated binding energy of accretion flows. No powerful outflows are present in CDAFs.
- CDAF is a very simple model which is now undergoing a rapid development. A more detailed account of plasma, magnetic, and radiative processes is likely to change this model.

## ACKNOWLEDGMENTS

The authors thank NORDITA and I.V.I. thanks Harvard-Smithsonian Center for Astrophysics for hospitality while part of this work was done. This work was supported by NSF grant PHY 9507695, the Royal Swedish Academy of Sciences, and RFBR grant 00-02-16135.

## REFERENCES

1. Bondi H., *MNRAS*, **112**, 195 (1952).
2. Shakura N.I., and Sunyaev R.A., *Astron. & Astrophys.*, **24**, 337 (1973).
3. Ichimaru S., *Astrophys. Journal*, **214**, 840 (1977).
4. Gilham S., *MNRAS*, **195**, 755 (1981).
5. Begelman M.C., and Meier D.L., *Astrophys. Journal*, **253**, 873 (1982).
6. Abramowicz M.A., Czerny B., Lasota J.-P., and Szuszkiewicz E., *Astrophys. Journal*, **332**, 646 (1988).
7. Narayan R., and Yi I., *Astrophys. Journal*, **428**, L13 (1994).
8. Abramowicz M.A., Chen X., Kato S., Lasota J.-P., and Regev O., *Astrophys. Journal*, **438**, L37 (1995).
9. Narayan R., and Yi I., *Astrophys. Journal*, **444**, 231 (1995).
10. Narayan R., and Yi I., *Astrophys. Journal*, **452**, 710 (1995).
11. Kato S., Fukue J., and Mineshige S., *Black-Hole Accretion Disks*, Kyoto: Kyoto Univ. Press (1998).
12. Abramowicz M.A., Blörnsson G., and Pringle J.E., *Theory of Black Hole Accretion Disks*, Cambridge: Cambridge Univ. Press (1998).
13. Xu G., and Chen X., *Astrophys. Journal*, **489**, L29 (1997).
14. Blandford R.D., and Begelman M.C., *MNRAS*, **303**, L1 (1999).
15. Ogilvie G.I., *MNRAS*, **306**, L9 (1999).
16. Abramowicz M.A., Lasota J.-P., and Igumenshchev I.V., *MNRAS*, **314**, 775 (2000).
17. Igumenshchev I.V., Chen X., and Abramowicz M.A., *MNRAS*, **278**, 236 (1996).
18. Igumenshchev I.V., and Abramowicz M.A., *MNRAS*, **303**, 309 (1999).
19. Stone J.M., Pringle J.E., and Begelman M.C., *MNRAS*, **310**, 1002 (1999).
20. Igumenshchev I.V., *MNRAS*, **314**, 54 (2000).
21. Igumenshchev I.V., Abramowicz M.A., and Narayan R., *Astrophys. Journal*, **537**, L27 (2000).
22. Igumenshchev I.V., and Abramowicz M.A., *Astrophys. Journal Sup.*, **130**, 463 (2000).
23. Ball G., Narayan R., and Quataert E., *Astrophys. Journal*, in press, astro-ph/0007037.
24. Narayan R., Igumenshchev I.V., and Abramowicz M.A., *Astrophys. Journal*, **539**, 798 (2000).
25. Quataert E., and Gruzinov A., *Astrophys. Journal*, **539**, 809 (2000).
26. Balbus S.A., and Hawley J.F., *Astrophys. Journal*, **376**, 214 (1991).
27. Matsumoto R., and Shibata K., in *Accretion Phenomena and Related Outflows*, ed. D. Wickramasinghe, G. Bicknell & L. Ferrario, ASP Conf. Ser. 121, 1997, p. 443.
28. Matsumoto R., in *Numerical Astrophysics*, ed. S. Miyama, K. Tomisaka & T. Hanawa, Dordrecht: Kluwer, 1999, p. 195.
29. Hawley J.F., *Astrophys. Journal*, **528**, 462 (2000).
30. Machida M., Hayashi M.R., and Matsumoto R., *Astrophys. Journal*, **532**, L67 (2000).
31. Machida M., Matsumoto R., and Mineshige S., *PASJ*, in press, astro-ph/0009004.
32. Stone J.M., and Pringle J.E., *MNRAS*, in press, astro-ph/0009233.